The role of rotation and kinetic damping in high-beta ST plasma stability

J.E. Menard[1], Y. Liu[2]
[1]*Princeton Plasma Physics Laboratory, Princeton, USA*
[2]*Culham Centre for Fusion Energy, Culham, UK*

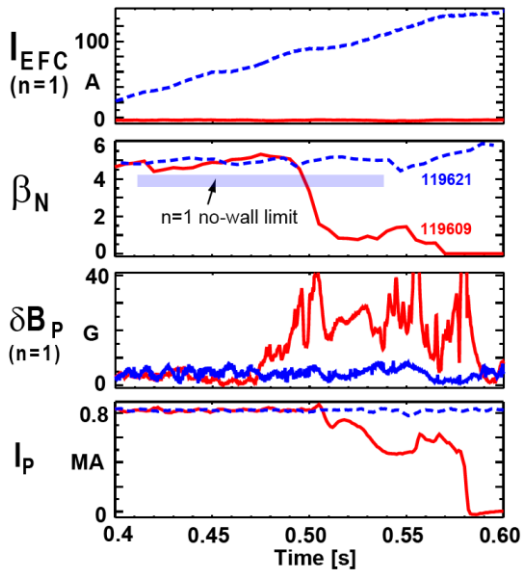

Figure 1- Comparison of NSTX plasmas in which an n=1 RWM is observed (red) versus a case with error field correction used to avoid RWM instability (blue).

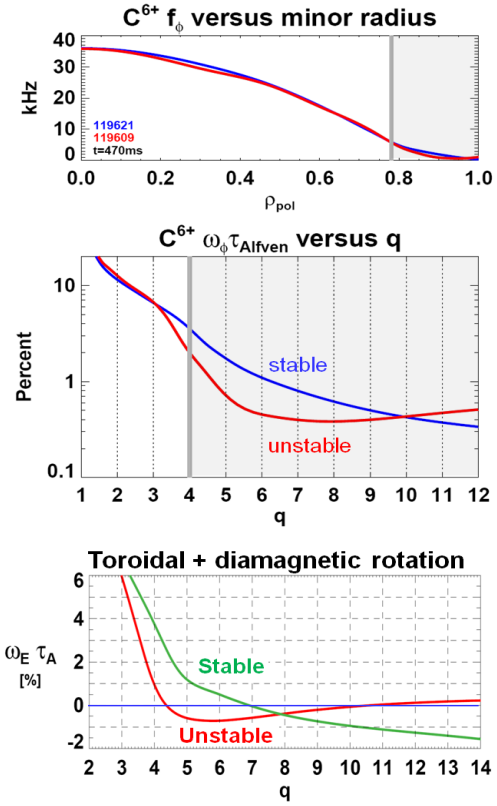

Figure 2 – Rotation profiles for RWM-stable (blue/green) and unstable (red) plasmas in NSTX.

Kinetic resonances have previously been identified to play an important role in the stability of the resistive wall mode (RWM) in high-beta NSTX plasmas operating above the ideal no-wall stability limit [1-4]. Most of the RWM stability calculations carried out thus far for NSTX have used the MISK code which utilizes a 'perturbative' approach to calculating RWM stability. In this approach, dissipation is computed using a non-rotating ideal-plasma eigenfunction at the marginal stability point. To begin to assess the impact of rotation and dissipation on RWM stability and eigenfunctions, kinetic MHD simulations have been performed using the MARS-F/K codes [5]. Further, for the first time, a systematic kinetic stability analysis of the with-wall limit (i.e. the stability of the 'plasma mode' [6]) has been carried out for NSTX. As for the RWM, the stability of the plasma mode is also found to be a sensitive function of rotation and dissipation.

Figure 1 shows the time evolution of parameters for otherwise identical high-β_N NSTX plasmas in which (red) an n=1 RWM is unstable and (blue) the addition of n=1 error field correction increases the edge toroidal rotation and avoids RWM instability [4]. A striking feature in these experiments is the apparently small difference in toroidal rotation profile for stable and unstable plasmas. The top two panels of Figure 2 shows that the difference in carbon impurity toroidal rotation occurs primarily in the last 20% of minor radius which corresponds to flux surfaces with q > 3. The bottom panel of Figure 2 shows the comparison of the ExB rotation frequency = ω_E profiles in which the diamagnetic contribution to the impurity rotation is included. This graph of Figure 2 also illustrates that the difference in RWM stability is apparently due to differences in rotation near the plasma edge on surfaces with q > 3.

MARS-F calculations of the stability of these plasmas using the semi-kinetic damping model with general-geometry corrections to the orbit times [4] are shown in Figure 3. At the time of RWM onset for the experimentally unstable equilibrium, the experimental operating operating point is predicted to be marginally unstable, and lower rotation and/or higher or lower beta are predicted to further drive instability. In contrast, for the experimentally stable case, there is a wide operating space in rotation and beta for which the plasma is predicted to be stable. Thus, the MARS-F calculations appear to have good overall consistency with the experiments.

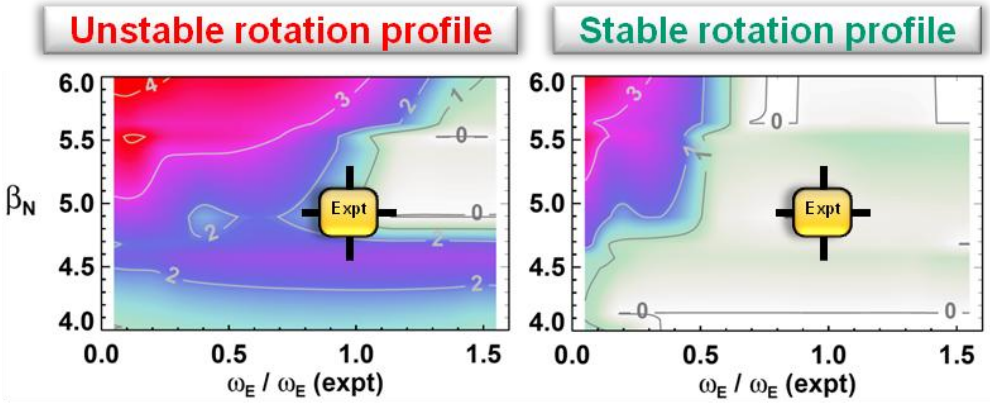

Figure 3 – n=1 RWM growth rate contours computed by MARS-F for the unstable rotation profile (left) from Figure 2, and for the stable profile (right). Contour level 0 represents stability, contour level 1 and higher represents instability.

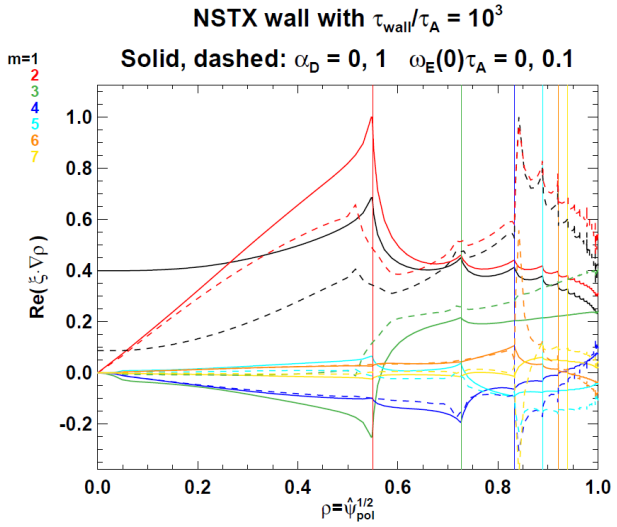

Figure 4 – MARS-K RWM eigenfunctions for the unstable plasma of Figures 1-3. The fluid (no rotation/dissipation) eigenfunction (solid) and the kinetic(dashed) cases are shown.

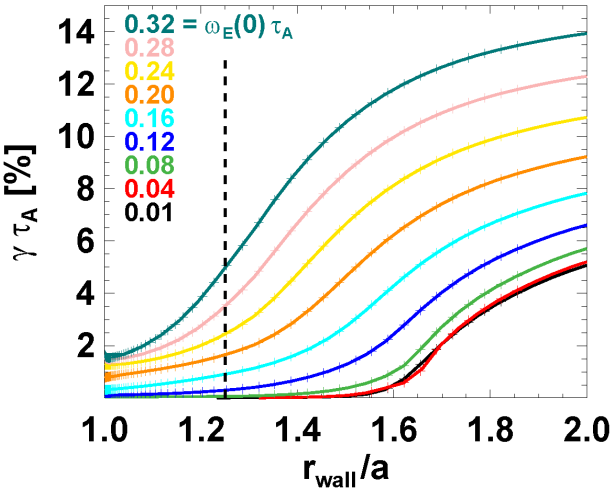

Figure 5 – Growth rate vs. conducting wall position and rotation frequency for the ideal 'plasma mode'.

MARS-K calculations for the same NSTX plasmas including the full drift-kinetic damping model (for both ions and electrons and including collisions) also predict the stable plasma to be stable and the unstable plasma to be unstable – i.e. consistency with the experiment. The MARS-K calculations also show that there can be substantial changes between the predicted fluid (non-kinetic) limit of the RWM eigenfunctions and the self-consistent eigenfunctions computed with rotation and kinetic damping included. As shown in Figure 4, the kinetic eigenfunction (dashed lines) with full damping and half the experimental rotation has much larger m=1-4 poloidal harmonic amplitudes of the normal displacement in the edge region than is the case for the ideal plasma eigenfunction. It is also noted that the displacement peaks can be shifted substantially away from the q=2 surface (vertical red line in Fig. 4) as the Alfvén singular points are split by Doppler shift induced by toroidal rotation [7].

Modifications to the RWM eigenfunction such as these could potentially impact the accuracy of the perturbative approach to calculating RWM stability, and this is an important topic for near-term investigation. Fundamentally, potentially large changes to the RWM eigenfunction result from the fact that the kinetic δW can be comparable to or larger in magnitude than the fluid δW components. These results also imply that in addition to determining RWM stability, rotation and dissipation effects might also influence 'plasma mode' [6] stability which determines the actual with-wall limit.

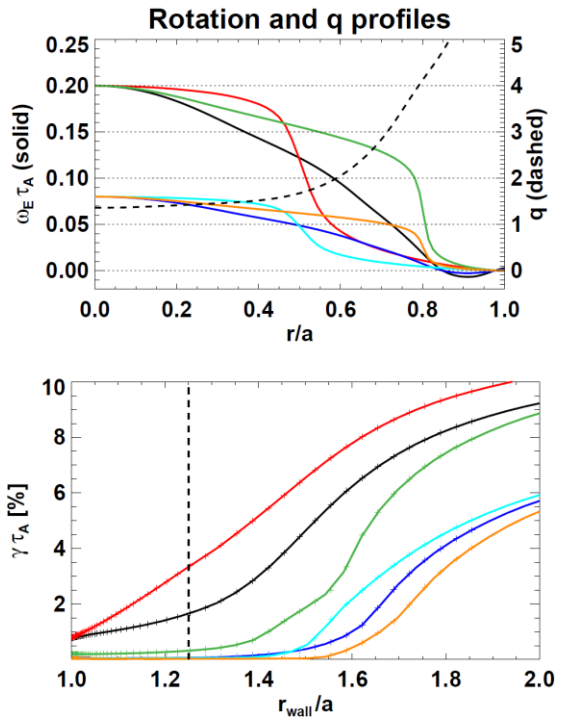

Figure 6 – Rotation profiles used to assess mode stability as a function of rotation and rotation shear.

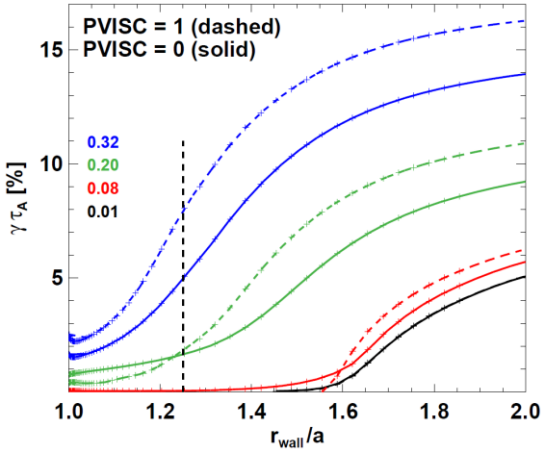

Figure 7 – Plasma mode growth rate vs. wall position and rotation for ideal MHD (solid) and with parallel sound-wave damping (dashed).

Figure 5 shows the stability of the plasma mode as a function of wall position and rotation scaled linearly from the experimental rotation profile. As is evident from Figure 5, at the lowest rotation value of $\omega_E(0)\tau_A$ = 0.01 the marginal wall position is r_{wall} / a ~ 1.6. As the rotation is increased toward $\omega_E(0)\tau_A$ = 0.1-0.12 in the absence of dissipation, the n=1 mode becomes unstable at the experimental nominal wall position of r_{wall} / a ~ 1.25 as indicated by the dashed vertical line in Figure 5. As the rotation is increased to $\omega_E(0)\tau_A$ = 0.2-0.3, the n=1 plasma mode is unstable even with the wall on the plasma boundary. This result is clearly inconsistent with the stable experimental discharge 119621 of Figures 1 and 3, and also apparently for the RWM-unstable shot 119609.

The rotation-driven instability shown in Figure 5 is is tentatively identified as a Kelvin-Helmholtz (KH) type instability [8]. To test this hypothesis, Figure 6 shows a set of rotation profiles used in MARS-K to calculate the n=1 mode growth rate as a function of wall position. The first set of profiles fixes $\omega_E(0)\tau_A$ = 0.2 and includes the experimental profile (black) and modified rotation profiles to vary the location of maximum shear to r/a = 0.5 (red) and 0.8 (green). As shown in Figure 6, increasing the rotation shear in the plasma core (red curves) increases the growth rate relative to the experimental profile – consistent with KH instability. However, increasing the rotation shear nearer to the plasma edge (green curves) significantly stabilizes the mode for r_{wall} / a < 1.4. Thus, the effects of rotation shear on mode stability depend on the location of maximum shear. The location of maximum shear impacts stability in a similar way for lower rotation $\omega_E(0)\tau_A$ = 0.08 as well as shown in the blue and orange curves of Figure 6.

Ideal MHD is known to incorrectly treat the parallel ion motion [9], and it is therefore possible that the destabilization driven by rotation shown in Figure 6 can be modified by kinetic damping. Figure 7 shows the impact of parallel sound-wave (SW) damping using a perturbed pressure relation of the form $\nabla\cdot\boldsymbol{\Pi}_1 = \kappa_{\|}\, \pi^{1/2}\, |k_{\|}v_{thi}|\, \rho \mathbf{v}_1\cdot\mathbf{bb}$ in the MARS momentum balance equation [6]. Here $\kappa_{\|}$ is a damping strength parameter and we choose $\kappa_{\|}$ = 0.56, i.e. PVISC $\equiv \kappa_{\|}\, \pi^{1/2}$ = 1 in MARS-F to simulate strong ion Landau damping which is comparable to ion Landau damping in the cylindrical tokamak limit (which would have $\kappa_{\|}$ = 1). As is evident from Figure 7, for large r_{wall} / a the inclusion of SW damping actually increases the mode growth rate. For smaller r_{wall} / a the growth-rate curves for SW damping intersect the ideal MHD curves and have lower growth rates – including complete stabilization for some cases such as for the $\omega_E(0)\tau_A$ = 0.08 case shown in red. For the experimental rotation $\omega_E(0)\tau_A$ = 0.2 and with conducting wall at the experimental location, SW damping changes the growth-rate very little, and the plasma is predicted to be unstable while the experiment is stable.

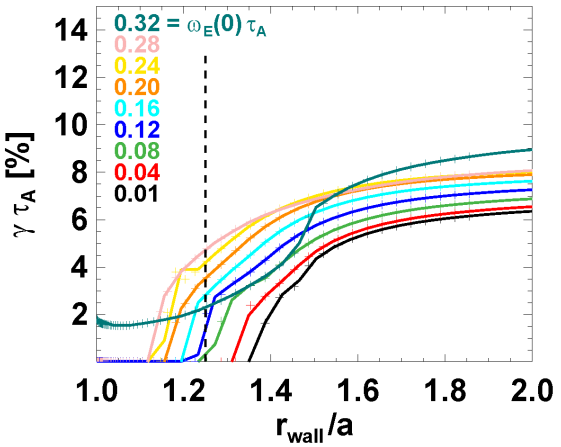

Figure 8 – Plasma mode growth rate vs. wall position and rotation using MARS-K kinetic damping model with only precession resonances included.

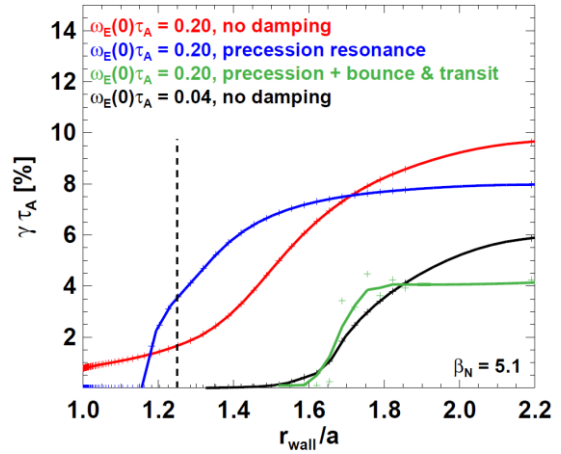

Figure 9 – Comparison of plasma mode growth rates for different damping models and rotation values.

Significantly different growth-rate dependencies on rotation and wall position are found using the full drift-kinetic perpendicular damping model implemented in MARS-K [5]. The perturbed kinetic pressures in MARS-K are velocity-space moments of terms proportional to λ_{ml} where

$$\lambda_{ml} = \frac{n[\omega_{*N} + (\hat{\epsilon}_k - 3/2)\omega_{*T} + \omega_E] - \omega}{n(\langle\omega_d\rangle + \omega_E) + [\alpha(m+nq) + l]\omega_b - i\nu_{\text{eff}} - \omega}$$

Including only the precession-drift resonance term $\langle\omega_d\rangle$ (i.e setting $\alpha(m+nq)+l = 0$), Figure 8 shows that the plasma mode can be stable over a wider range of rotation, but only at reduced r_{wall} / a < 1.4 even at low rotation. In particular, for this damping model, the critical wall position at low rotation $\omega_E(0)\tau_A = 0.01$ is 1.35 compared to 1.6 for the ideal plasma result as shown in Figure 5. In addition, the mode growth rate is generally reduced for large r_{wall} / a relative to ideal plasma predictions. Figure 8 also shows that the mode can remain stable at high $\omega_E(0)\tau_A$ at small r_{wall} / a, but ultimately at sufficiently high $\omega_E(0)\tau_A \sim 0.3$, the plasma is unstable even for r_{wall} / a = 1. For this damping model, the plasma is again predicted to be unstable at the experimental rotation and wall position, but the experiment is stable.

The green curve in Figure 9 shows the result of MARS-K simluations including all kinetic resonance terms - i.e $\alpha(m+nq)+l \neq 0$ in λ_{ml} above. The simulations indicate that including both the precession and bounce and transit resonances for the experimental $\omega_E(0)\tau_A \sim 0.2$ significantly increases the plasma mode stability. In particular, the critical wall position increases to 1.6 as compared to 1.15 obtained if only the precession resonances are included (blue curve). The plasma mode calculation including full kinetic damping is also more stable than the ideal plasma case (red curve) which is unstable even with a wall on the plasma boundary. Interestingly, the marginal wall position r_{wall} / a = 1.6 utilizing the full kinetic damping model is similar to the low-rotation ideal plasma value (black curve). Additional work is needed to determine if this is just a coincidence, or is a more general result. Most importantly, these results indicate that only the full kinetic damping model is consistent with the observed plasma mode stability of the experiment. The influence of increased beta and rotation will be studied in future work to determine the with-wall limit using the full kinetic damping model to compare to the experimental with-wall limit. This work is supported by U.S. DOE Contract DE-AC02-09CH11466.

References

[1] J. W. Berkery, et al., Phys. Rev. Lett. **104**, 035003 (2010)
[2] J. W. Berkery, et al., Phys. Plasmas **17**, 082504 (2010)
[3] S.A. Sabbagh, et al., Nucl. Fusion **50** 025020 (2010)
[4] J.E. Menard, et al., Nucl. Fusion **50** 045008 (2010)
[5] Y.-Q. Liu, et al., Phys. Plasmas **15**, 112503 (2008)
[6] M.S. Chu, et al., Phys. Plasmas **2**, 2236 (1995)
[7] J. Shiraishi, et al., Phys. Plasmas **17**, 012504 (2010)
[8] I.T. Chapman, et al, Plasma Phys. Control. Fusion **53** ,125002 (2011)
[9] A. Bondeson and R. Iacono, Phys. Fluids B **1**, 1431(1989)